

Automatic Segmentation of Multicellular Tumour Spheroids Images During Growing

Original

Automatic Segmentation of Multicellular Tumour Spheroids Images During Growing / Introvaia, Alessandra; Muccio, Sara; Bezze, Andrea; Mattu, Clara; Balestra, Gabriella. - ELETTRONICO. - 321:(2024), pp. 230-234. (Intervento presentato al convegno European Federation for Medical Informatics Special Topic Conference (EFMI STC) 2024 - Collaboration across Disciplines for the Health of People, Animals and Ecosystems tenutosi a Timisoara (RO) nel 27 to 29 November 2024) [10.3233/shti241098].

Availability:

This version is available at: 11583/2994745 since: 2024-11-24T19:11:44Z

Publisher:

IOS Press

Published

DOI:10.3233/shti241098

Terms of use:

This article is made available under terms and conditions as specified in the corresponding bibliographic description in the repository

Publisher copyright

(Article begins on next page)

Automatic Segmentation of Multicellular Tumour Spheroids Images During Growing

Alessandra INTROVAIA^a, Sara MUCCIO^b, Andrea BEZZE^b, Clara MATTU^b and Gabriella BALESTRA^{a,1}

^aDepartment of Electronics and Telecommunications– Politecnico di Torino, Italy

^bDepartment of Mechanical and Aerospace Engineering – Politecnico di Torino, Italy

ORCID ID: Alessandra Introvaia <https://orcid.org/0009-0003-6526-7697>, Sara Muccio <https://orcid.org/0009-0002-1757-7597>, Andrea Bezze <https://orcid.org/0000-0002-8061-5034>, Clara Mattu <https://orcid.org/0000-0002-3969-8771>, Gabriella Balestra <https://orcid.org/0000-0003-2717-648X>

Abstract. Image segmentation is an important topic in medical image processing. Multicellular tumour spheroids (MTS) are currently one of the most widely employed *in vitro* model for pre-clinical drug screening in cancer research. Assessing their growing requires the segmentation of images acquired at several time points. This paper presents the preliminary results of an approach for the automatic segmentation of multicellular tumour spheroids. The obtained segmentation accuracy is reasonable demonstrating that the approach proved adequate.

Keywords. Spheroids, 3D cellular spheroids, Image segmentation, Image processing, Level-set, Region Growing

1. Introduction

The domain of image processing is characterised by a number of challenges, including the time-consuming and operator-dependent nature of the process, inter- and intra-operator variability, and limited scalability. To address these issues, a range of automated image processing methods have been proposed, encompassing traditional (or heuristic) algorithms and artificial intelligence (AI)-based techniques. In this context, *Lacalle et al.* [1] proposed SpheroidJ, an open-source tool for the segmentation of spheroid images. Specifically, it employs a binarization algorithm and contour detection based on the Sobel edge detection operator to segment images of human glioblastoma spheroids. Furthermore, *Chen et al.* [2] developed SpheroidSizer, a MATLAB-based tool for spheroid segmentation that employs a Chan-Vese level-set algorithm. Additionally, it enables the extraction of quantitative parameters (e.g., area, width, length, and volume). Recently, there was an increasing of the application of AI techniques for image segmentation, driven by advancements in computational power. In the specific field of spheroid image segmentation, *Grexa et al.* [3] and *Akshay et al.* [4] presented two notable deep learning (DL) frameworks that perform the segmentation task using Mask R-CNN

¹ Corresponding Author: Gabriella Balestra; E-mail: gabriella.balestra@polito.it.

networks. Specifically, SpheroidPicker employs a ResNet-101 backbone and is trained on bright-field RGB images; in contrast SpheroScan uses a ResNet-50 feature pyramid network as a backbone and it is trained on spheroids composed of bladder smooth muscle cells (SMCs) and human embryonic kidney (HEK) cells. In several studies, both traditional and artificial intelligence-based algorithms have been integrated into a segmentation tool. Indeed, *Piccinini et al.* [5] proposed AnaSP, a MATLAB-based platform that deploys both traditional thresholding techniques and deep learning algorithms based on convolutional neural networks (CNN), including VGGs and ResNets.

Multicellular tumour spheroids (MTS) are currently one of the most widely employed *in vitro* model for pre-clinical drug screening in cancer research [7]. These three-dimensional cell aggregates are not attached to any surface and are composed of heterogeneous mixtures of different cell types. A significant potentiality of MTSs resides in their ability to replicate the physiologically relevant spatial configuration of different tumours such as glioblastoma multiforme (GBM) and to allow precise adjustments to their composition, offering a realistic platform for drug screening [8]. MTSs allows the study of interactions among various cell types within the tumour microenvironment, including immune, stromal, and endothelial cells. Additionally, they can replicate hypoxic and necrotic regions found in tumours. While traditional drug screening on MTSs involves destructive colorimetric viability tests, there is a growing interest in using images acquired through optical and fluorescence microscopy as label-free systems to assess treatment efficacy [9]. In addition, MTS are often characterized by an intrinsic variability in shape and size, correlated to the formation protocol adopted or culturing conditions. In this optic, it is imperative to develop reliable tools to identify not only the best conditions for the pre-selection of the best spheroids, but also the pivotal parameters that can better evaluate spheroids behaviour [7]. Studies have demonstrated that various morphological parameters, such as size, circularity, invasion area, and optical density, can be extracted from optical images to describe treatment responses [10]. However, the accuracy of these parameters heavily relies on the quality of image segmentation. To facilitate the study of MTSs and provide reliable high-throughput screening platforms, it is crucial to develop image processing algorithms for automatic segmentation and parameter extraction. Current segmentation methods are often optimized for analysing single MTSs in suspension culture and may not generalize well to different experimental conditions, such as studying MTS infiltration patterns within hydrogel matrices.

The aim of this paper is to present the preliminary results of a method for the automatic segmentation of multicellular tumour spheroids.

2. Spheroid Segmentation

2.1 Dataset description

The dataset employed in this work consists of fluorescent spheroids images acquired using spinning disk microscope (Nikon Eclipse Ti 2), with 10x magnification. Mature Tumour Mix spheroids (composed by 90% U87-GFP and 10% GBM-8-GFP cells) were prepared using Corning® Costar® Ultra-Low Attachment Multiple 96-wells Plate (Merck) (4000 cells/well) and embedded in a Glioma extracellular matrix (G-ECM)-gel solution, composed by collagen-I hydrogel (4mg/mL), in a 96 well plate. The 96-wells

plate was then placed in incubator at 37°C for at least 15 minutes to allow the jellification. To explore the role of microglia cells in supporting tumour spheroids invasion, Tumour Mix (with U87-GFP and GBM-8-GFP) spheroids were embedded in the G-ECM hydrogel, as well as single microglia cells (e.g. HMC3 cells) (100 cells/ μ l, for a total volume of 10 μ l per well). Both types of spheroids were divided into different treatment groups as follows:

- A control spheroid (CTRL), which is not treated with any drugs, and it is used as reference;
- Free Drug (FD)-treated spheroids, which are treated with different concentrations (10, 50 and 200 nM) of Bortezomib delivered as free drug;
- Nanoparticles (NPs)-treated spheroids, which are treated with the same concentrations of Bortezomib but encapsulated in nanoparticles;

Tumour Spheroids were treated after 24h post transfer, to let the spheroids adapt to the new culture conditions. In order to evaluate the effect of each treatment, an image of each spheroid was captured each spheroid was imaged at five different time-steps: 0, 24, 48, 72, and 96 hours. Overall, the dataset comprises 205 images, each with a resolution of 1608x1608 pixels with a pixel intensity range of 0-255 (uint8 format). Segmentation was performed on each image with a fixed threshold by a researcher using the microscope itself, and these masks were used as a reference.

2.2 Methods

In this work, we propose a two-steps approach for spheroids images segmentation, developed on MATALB (version R2023b). This approach allows to distinguish between two main components of these cellular models (i.e., core and branches) that provide different information. Specifically, the two phases are developed using a level-set (LS) algorithm followed by a region-growing (RG) algorithm. Lastly, post-processing operations are performed.

The first step of our segmentation pipeline encompasses a LV algorithm based on the Chan-Vese model [6], an active contour-based method able to detect objects through a curve evolution. To address the high computational costs of the LV model, caused by the high images size, they are initially resized by a shrink factor of 10. With respect to the initialisation of the contour, first the maximum point of the image gradients is calculated, and this point is identified as seed; second, a circumference centred on the seed is defined. The contour movement is driven by energy, modelled using intensity and regularisation terms, which practically depends on the value of a parameter (i.e., the alpha parameter). To identify the optimal value, we have segmented the images using different values of alpha and, at the end, we set alpha equal to 6.

The second step of our approach employs a RG algorithm for spheroid branches segmentation, using the pixels segmented in the former stage as the initial seeds. In this context, we optimise the parameters related to neighbourhood size and shape and introduce contrast enhancement. Precisely, we have evaluated five possible neighbourhoods: squares of sizes 3, 9, and 27, and discs with radii of 9 and 27. This analysis ensures that the branches are accurately captured, reflecting their true extensions and connections to the core. As a result of this assessment, the algorithm was carried out with the 27-pixel radius disc and 80% of contrast enhancement.

To refine the segmentation masks, post-processing operations are performed. Among these are filling holes and removing small objects. In addition, the possibility of

keeping only the largest segmented object is considered, although this assumption is not always verified.

2.3 Preliminary Results

Figure 1 shows the segmentation results of the NPs 10 nM MIX spheroid across the five time-steps. Each sub-figure is divided into two rows: the first one displays the segmentation on the original images, while the latter refers to the contrast-enhanced images. The contours depicted include those from the LV algorithm, RG with square neighbourhoods of sizes 3, 9, and 27, RG with circular neighbourhoods of radii 9 and 27, and the reference obtained using the microscope. It can be noticed that larger neighbourhoods enable the segmentation of further areas of the spheroid branches. Additionally, for a given neighbourhood size, contrast enhancement allows for the detection of more peripheral regions of the spheroid.

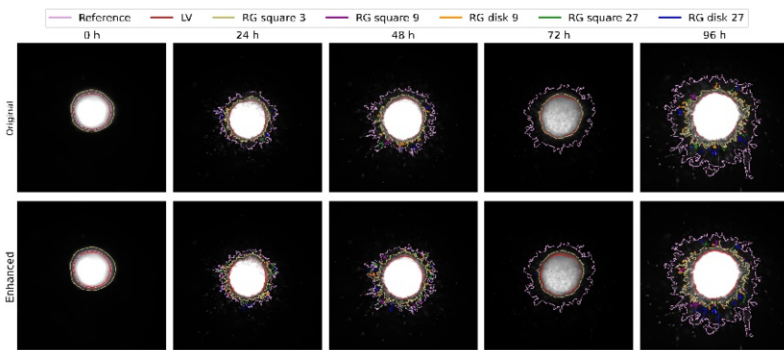


Figure 1. Segmentation results on NPs 10 nM spheroid over time.

Figure 2 presents the boxplots of Dice, Jaccard, Precision, and Recall for the time intervals under analysis. These metrics were computed between the reference masks and the RG masks obtained with 27-pixel radius disc as neighbourhood and 80% of image contrast enhancement. The results at time-step 0h are the highest and exhibit minimal variability, in part due to the circular shape of the spheroid with few branches. From 24h onwards, the results are lower than at the initial time-step. Nevertheless, the Dice scores show mean values around 80%, while the Jaccard average values are around 70%. In sub-figures C and D, it can be observed that Precision values are approximately 1 in all time-steps, whereas the Recall value are lower. These results suggest that our algorithm tends to under-segment the spheroids in comparison to the reference. This can be justified as the reference masks obtained using the microscope are notably over-estimated.

3. Conclusions

The paper presents the results of the segmentation of 205 images that document the growing of 41 spheroids. The segmentation accuracy is reasonable. The performances of the proposed approach will be further assessed on a larger dataset.

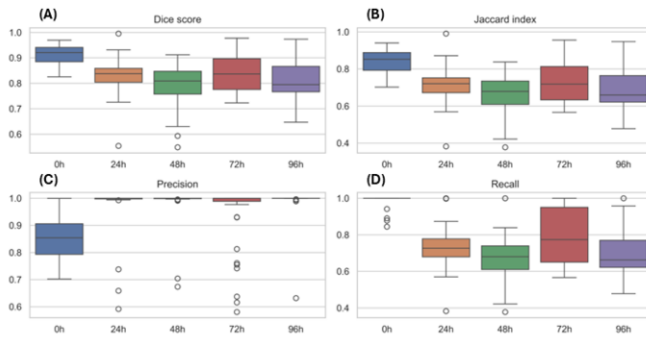


Figure 2. Dice, Jaccard, Precision and Recall metrics computed.

Acknowledgements

The research scholarship of Alessandra Introvaia is supported by the project POC NAPTER NODES which has received funding from the MUR – M4C2 1.5 of PNRR funded by the European Union - NextGenerationEU (Grant agreement no. ECS00000036). Sara Muccio acknowledges “JUST THE WOMAN I AM 2023” for founding her research fellowship.

References

- [1] Lacalle D, Castro-Abril HA, Randelovic T, Domínguez C, Heras J, Mata E, et al. SpheroidJ: An Open-Source Set of Tools for Spheroid Segmentation. *Computer Methods and Programs in Biomedicine*. 2021 Mar; 200:105837. doi: 10.1016/j.cmpb.2020.105837
- [2] Chen W, Wong C, Vosburgh E, Levine AJ, Foran DJ, Xu EY. High-throughput Image Analysis of Tumor Spheroids: A User-friendly Software Application to Measure the Size of Spheroids Automatically and Accurately. *JoVE*. 2014 Jul 8;(89):51639, doi: 10.3791/51639
- [3] Grexa I, Diosdi A, Harmati M, Kriston A, Moshkov N, Buzas K, et al. SpheroidPicker for automated 3D cell culture manipulation using deep learning. *Sci Rep*. 2021 Jul 20;11(1):14813, doi: 10.1038/s41598-021-94217-1
- [4] Akshay A, Katoch M, Abedi M, Shekarchizadeh N, Besic M, Burkhard FC, et al. SpheroScan: a user-friendly deep learning tool for spheroid image analysis. *GigaScience*. 2022 Dec 28;12:giad082, doi: 10.1093/gigascience/giad082
- [5] Piccinini F. AnaSP: A software suite for automatic image analysis of multicellular spheroids. *Computer Methods and Programs in Biomedicine*. 2015 Apr;119(1):43–52, doi: 10.1016/j.cmpb.2015.02.006
- [6] Chan TF, Vese LA. Active contours without edges. *IEEE Trans on Image Process*. 2001 Feb;10(2):266–77, doi: 10.1109/83.902291
- [7] Zononi, M., Piccinini, F., Arienti, C. et al. 3D tumor spheroid models for in vitro therapeutic screening: a systematic approach to enhance the biological relevance of data obtained. *Scientific Reports*. 2016 January; 6(1):1–11, doi: 10.1038/srep19103
- [8] Guyon J, Andrique L, Pujol N, Røslund GV, Recher G, Bikfalvi A, et al. A 3D Spheroid Model for Glioblastoma. *Journal of Visualized Experiments*. 2020 April; 9:(158). doi: 10.3791/60998
- [9] Costa EC, Moreira AF, de Melo-Diogo D, Gaspar VM, Carvalho MP, Correia IJ. 3D tumor spheroids: an overview on the tools and techniques used for their analysis. *Biotechnol Adv*. 2016 December;34(8):1427–41, doi: 10.1016/j.biotechadv.2016.11.002
- [10] Thakuri PS, Gupta M, Plaster M, Tavana H. Quantitative Size-Based Analysis of Tumor Spheroids and Responses to Therapeutics. *Assay and Drug Development Technologies*. 2019 April;17(3):140-149, doi: 10.1089/adt.2018.895